

Modeling $p\text{CO}_2$ variability in the Gulf of Mexico

Published by Copernicus Publications on behalf of the European Geosciences Union.

ferent seasons (e.g., Lohrenz et al., 2010 for the northern Gulf of Mexico; Jiang et al., 2008 for the South Atlantic Bight; Signorini et al., 2013 for the North American east coast; Tsunogai et al., 1999 for the East China Sea). Quantifying the ocean carbon budget is therefore a difficult task.

5 Our study focuses on the carbon cycle in the Gulf of Mexico (GoM). One unique feature of the gulf environment is that it receives enormous riverine nutrient and carbon inputs, the majority of which are from the Mississippi/Atchafalaya River system. Excessive nutrient and carbon loading causes coastal eutrophication, which triggers not only the well-known hypoxia phenomenon (a.k.a. the “Dead Zone”, Rabalais et al., 2002),
10 but also a newly revealed coastal ocean acidification problem (Cai et al., 2011). However, the carbon budget associated with such enormous terrestrial carbon and nutrient inputs still remains unclear: on the one hand extensive riverine carbon input results in over-saturated coastal waters, which serve as a CO₂ source to the atmosphere (e.g. Lohrenz et al., 2010; Guo et al., 2012); on the other hand, although the Mississippi River Plume region is a heterotrophic system that breaks down organic carbon (Murrell et al., 2013), enhanced primary production in the river plume due to significant inputs of inorganic nutrients would introduce a net influx of CO₂. Further offshore, the circulation in the GoM is largely influenced by the energetic Loop Current. Large anticyclonic eddies periodically pinch off from the Loop Current (Sturges and Leben,
20 2000) and, along with the cross-shelf circulation driven by wind and other meso-scale and submeso-scale coastal processes, enhance material exchanges between the eutrophic coastal waters and oligotrophic deep-ocean waters (e.g., Toner et al., 2003). Indeed, a recent observational study suggested significant dissolved inorganic carbon (DIC, $\sim 3.30 \times 10^{12}$ mol C yr⁻¹) export from the GoM shelf to the Loop Current waters
25 (Wang et al., 2013).

While global inorganic carbon budgets have been made available through joint seawater CO₂ observations (e.g. World Ocean Circulation Experiment and Joint Global Ocean Flux study, Sabine et al., 2004; Feely et al., 2004; Orr et al., 2005), they are too coarse to resolve the GoM (Gledhill et al., 2008). Regional carbon assessments for the

12675

GoM were made recently based on limited in situ observations (e.g. Cai, 2003; Lohrenz et al., 2010; Huang, 2013 focused on the Mississippi River plume and the Louisiana Shelf; Wang et al., 2013 covered three cross-shelf transects in the northeastern GoM but only for one summer). Significant uncertainties exist in such budget estimations
5 due to large temporal and spatial gaps present in the observations (e.g. Coble et al., 2010; Hofmann et al., 2011; Robbins et al., 2014). In this regard, coupled physical–biogeochemical models capable of representing the biogeochemical cycle with realistic physical settings (e.g., ocean mixing and advection) provide an alternative means for the budget assessment.

10 Here we present a *p*CO₂ analysis for the GoM based on the results of a coupled physical–biogeochemical model simulation. Our objective is to quantify the *p*CO₂ flux at the air–sea interface (which at present is highly uncertain when based on observational analyses alone), with specific emphasis on its variability in relationship with river plume dynamics and dominant oceanic processes in different regions of the GoM.

15 2 Method

Our analysis uses solutions from a coupled physical–biogeochemical model covering the GoM and South Atlantic Bight waters (Xue et al., 2013). The circulation component of the coupled model is the Regional Ocean Modeling System (ROMS, Haidvogel et al., 2008; Shchepetkin and McWilliams, 2005) and is coupled with the biogeochemical module described in Fennel et al. (2006, 2008, and 2011). A seven year (1 January 2004–31 December 2010) hindcast was performed with the system, driven by realistic atmospheric forcing (North America Regional Reanalysis, www.cdc.noaa.gov), open boundary conditions from a data-assimilative global ocean circulation model (HYCOM/NCODA, Chassignet et al., 2007), and observed freshwater and terrestrial nutrient input from 63 major rivers (Aulenbach et al., 2007; Milliman and Farnsworth,
25 2011; Fuentes-Yaco et al., 2001; Nixon, 1996). Model validations (physics, nutrients and chlorophyll) and a nitrogen budget have been reported in Xue et al. (2013).

12676

In this study we focus on the carbon cycle in the GoM. As before, we considered the first year of the simulation (2004) as model spin-up; all results presented here are for model output from 2005 to 2010. The carbonate chemistry of the coupled model is based on the standard defined by the Ocean Carbon Cycle Model Intercomparison Project Phase 2 (Orr et al., 2000). There are two active tracers, DIC and alkalinity, to determine the other four variables of the carbonate system (i.e. $p\text{CO}_2$, carbonate ion concentration, bicarbonate ion concentration, and pH; Zeebe and Wolf-Gladrow, 2001). The initial and open boundary conditions of DIC and alkalinity in the open ocean ($> 200\text{ m}$ water depth) are prescribed based on their relationship with salinity and temperature as derived by Lee et al. (2000, 2006). In the coastal and shelf waters ($< 200\text{ m}$), initial values of DIC and alkalinity were defined using a relationship among salinity, DIC and alkalinity based on data collected on the Louisiana Shelf (Cai, 2011). The carbon cycle parameterization used in the hindcast followed the same approach and values as in Fennel et al. (2008), Fennel and Wilkin (2009) and Fennel (2010).

To account for riverine input into the model domain, we constructed climatological monthly time series of alkalinity by averaging all available US Geological Survey alkalinity observations for each major river. Because direct riverine DIC measurements were not available, we approximated river DIC input using the corresponding alkalinity value plus 50, following Guo et al. (2012). The fluvial DIC input to the GoM was estimated as $\sim 2.18 \times 10^{12} \text{ mol C yr}^{-1}$, the majority of which was delivered by the Mississippi/Atchafalaya River ($\sim 1.80 \times 10^{12} \text{ mol C yr}^{-1}$, comparable with the estimation in Cai, 2003). The gas exchange calculation follows Wanninkhof (1992). The temporal variation of air $p\text{CO}_2$ is prescribed using the following curve-fitting model provided by the Cooperative Global Atmospheric Data Integration Project:

$$p\text{CO}_{2\text{air_secular}} = 282.6 + 0.125 \times \text{pmonth} \times 12 - 7.18 \times \sin(\pi/2 \times \text{pmonth} + 0.86) - 0.99 \times \sin(\pi/2 \times \text{pmonth} + 0.28) - 0.80 \times \sin(\pi/2 \times \text{pmonth} + 0.06) \quad (1)$$

12677

where $p\text{CO}_{2\text{air_secular}}$ represents the secular monthly air $p\text{CO}_2$; pmonth represents the months since January 1951, and $\pi/2$ is a constant equal to 6.28. Air $p\text{CO}_2$ was set to be spatially uniform.

3 Results

In this section, we present model-simulated sea surface $p\text{CO}_2$ and model-estimated air-sea CO_2 flux in different sub-regions of the GoM. In situ data from various sources were included for model validation. Because large $p\text{CO}_2$ gradients were found in both in-situ data and model in shallow waters, in-situ and model data for waters with $< 10\text{ m}$ depth were excluded.

3.1 Sea surface $p\text{CO}_2$

Spatially averaged model-simulated $p\text{CO}_2$ on the Louisiana Shelf exhibited clear seasonality, with large values ($\sim 500\text{ ppm}$) around August and smallest values ($\sim 350\text{ ppm}$) around February (Fig. 1a, area map see Fig. 2). Gulf-wide spatially averaged $p\text{CO}_2$ (Fig. 1b) had a temporal pattern similar to that on the Louisiana Shelf, with high $p\text{CO}_2$ values ($\sim 450\text{ ppm}$) in August and low values ($\sim 250\text{ ppm}$) in February. The $p\text{CO}_2$ on the Louisiana Shelf was generally 100 ppm higher than that in the entire gulf.

For model validation, we used in situ measurements collected on the Louisiana Shelf (Huang, 2013; Huang et al., 2013). These ship-based observations were taken in October 2005; April, June, August 2006; May, August 2007; January, April, July, November 2009; and March 2010, respectively. To alleviate the spatial and temporal heterogeneity associated with these in-situ data (see Huang, 2013 for data distribution), we overlaid the mean value of in situ measurements during each survey over the model-simulated $p\text{CO}_2$ time series (Fig. 1a). On the Louisiana Shelf, our model was able to capture the measured $p\text{CO}_2$ in 6 out of the 11 cruises. Specifically, agreement between model and observations was better during spring, including April 2006, May 2007,

12678

April 2009, and March 2010, than summer, including June 2006, August 2007, and July 2009, when $p\text{CO}_2$ was overestimated. The overall overestimated $p\text{CO}_2$ during summer months will be discussed later.

On a gulf-wide extent, the LDEO in situ data were grouped by a 10 day temporal window (> 180000 data points gulf-wide during 2005–2010; Takahashi et al., 2013) and overlaid on the spatially averaged $p\text{CO}_2$ time series for the entire gulf (Fig. 1b). The in situ data exhibited a similar seasonality with that reproduced by the model and 32 out of the 40 data groups were within one standard deviation of the modeled time series. The above-mentioned comparisons indicate that our coupled physical–biogeochemical model is capable of resolving gulf-wide seasonal and intra-annual variations in observed $p\text{CO}_2$, allowing us to use this seven-year hindcast to further characterize the air–sea CO_2 flux.

3.2 Air–sea CO_2 flux

To facilitate our description of the air–sea CO_2 flux, the GoM was divided into five sub-regions: (1) Mexico Shelf, (2) Texas Shelf, (3) Louisiana Shelf, (4) West Florida Shelf, and (5) open ocean (Fig. 2; following the regional definitions in Benway and Coble, 2014).

Based on model simulations, the GoM was characterized as an overall CO_2 sink with a multi-year mean (2005–2010) carbon flux rate of $0.86 \text{ mol C m}^{-2} \text{ yr}^{-1}$ ($\sim 1.34 \times 10^{12} \text{ mol C yr}^{-1}$, Table 1 and Fig. 2). Examining region by region, we see that the open ocean, occupying $\sim 65\%$ of the GoM in area, acts as a CO_2 sink ($1.06 \text{ mol m}^{-2} \text{ yr}^{-1}$ of C) during most of the year except in summer. The greatest carbon uptake occurred in winter ($2.24 \text{ mol C m}^{-2} \text{ yr}^{-1}$). From a closer examination of the CO_2 flux map, it was evident waters around the Loop Current were a continuous sink, while the western part of the open ocean shifted between acting as a source in summer and fall and a sink in winter and spring.

Compared with the open ocean, air–sea flux on the continental shelf was more location-dependent and varied from season to season. Among the four shelf sub-

12679

regions, the Mexico Shelf has the largest area. It acted as a strong carbon sink in winter and spring (2.25 and $1.76 \text{ mol C m}^{-2} \text{ yr}^{-1}$) and a weaker sink in summer and fall (0.03 and $0.31 \text{ mol C m}^{-2} \text{ yr}^{-1}$). Waters along the eastern side of the Mexico Shelf were a sink during most of the year, while to the west the ocean was a source in summer and fall. On a yearly scale, this region was a sink with an air–sea flux of $1.09 \text{ mol C m}^{-2} \text{ yr}^{-1}$. To the north, the Texas Shelf has the smallest area among the four shelf sub-regions. It acted as a CO_2 source during spring, summer, and fall (-0.03 , -1.15 and $-0.46 \text{ mol C m}^{-2} \text{ yr}^{-1}$) and a strong sink during winter ($1.89 \text{ mol C m}^{-2} \text{ yr}^{-1}$). On a yearly scale this region was a weak CO_2 sink with an air–sea flux of $0.06 \text{ mol C m}^{-2} \text{ yr}^{-1}$.

The Louisiana Shelf shifted between acting as a CO_2 source in summer and fall (-1.47 and $-0.41 \text{ mol C m}^{-2} \text{ yr}^{-1}$) and a sink in winter and spring (2.59 and $0.99 \text{ mol C m}^{-2} \text{ yr}^{-1}$). The most prominent feature here is the continuous, strong degassing in the coastal waters around the Mississippi–Atchafalaya River mouths. The open shelf shifted from acting as a sink during winter and spring to a source during summer and fall. Despite the extensive degassing in the coastal water, the Louisiana Shelf overall was a CO_2 sink on a yearly basis ($0.42 \text{ mol C m}^{-2} \text{ yr}^{-1}$). Similarly, the West Florida Shelf also shifted from acting as a CO_2 source in summer and fall (-1.06 and $-1.28 \text{ mol C m}^{-2} \text{ yr}^{-1}$) to a sink in winter and spring (1.41 and $0.49 \text{ mol C m}^{-2} \text{ yr}^{-1}$). The degassing in the inner shelf is strong enough to make the West Florida Shelf a CO_2 source on a yearly basis ($-0.11 \text{ mol C m}^{-2} \text{ yr}^{-1}$).

Despite the salient spatial and temporal variability, the GoM was an overall CO_2 sink, mainly because of the strong uptake in the open ocean. For validation purposes, we compared (in Table 1) the model-simulated air–sea flux against an estimation based on observations, which utilized all available measurements collected within the GoM from 2005 to 2010 (Robbins et al., 2014). Our control-run estimation agrees with the in situ measurements in all five sub-regions in terms of the ocean’s role as a CO_2 source or sink. There is some discrepancy in the magnitude of the estimated flux on the Mexico Shelf and in the open ocean, which can be attributed to the spatial and

temporal heterogeneity of the in situ dataset (see distributions in Takahashi et al., 2013) and warrants further investigation.

3.3 No-bio simulation

To test biological processes' role in regional $p\text{CO}_2$ variability, a no-bio simulation was conducted, where all biology sources and sinks of DIC and alkalinity were disabled similar to the experiment described in Fennel and Wilkin (2009). Surface $p\text{CO}_2$ was elevated in the no-bio simulation where the biological sources and sinks of carbon were disabled. The multi-year mean $p\text{CO}_2$ was increased from 402.1 to 453.3 ppm for the Louisiana Shelf and from 358.0 to 428.2 ppm for the entire gulf (Fig. 1). Nevertheless, such $p\text{CO}_2$ increase was not temporally uniform. Specifically on the Louisiana Shelf, $p\text{CO}_2$ increases in the no-bio simulation was clear higher during spring-summer than during fall-winter. For air-sea flux, the elevated surface $p\text{CO}_2$ (~ 70 ppm for the entire gulf) turn all five sub-regions into to a strong carbon source, resulting in a net outflux of $1.57 \text{ mol C m}^{-2} \text{ yr}^{-1}$ (Table 1).

4 Discussion

This study provides an unprecedented model simulation of carbon fluxes and exchanges in the Gulf of Mexico. Until recently, carbon dynamics in the Gulf of Mexico have been poorly characterized and represented a large source of uncertainty in regional carbon budgets. Here, we examine the model-simulated spatial and temporal patterns in air-sea flux of CO_2 and discuss the factors controlling $p\text{CO}_2$ variability in different subregions of the GoM with specific focus on the river-influenced Louisiana Shelf and the Loop Current-influenced open ocean. The relationship between $p\text{CO}_2$ and other hydrographic variables are also considered.

12681

4.1 Factors controlling spatial distribution of surface $p\text{CO}_2$

The Mississippi-Atchafalaya River and associated plume play the most important role in determining the $p\text{CO}_2$ distribution on the Louisiana Shelf. A large input of fluvial DIC and alkalinity introduce carbonate saturation in the coastal waters, conversely, nutrients from the river enhance local primary production, which results in DIC removal and thus reduces seawater $p\text{CO}_2$ (e.g. Lohrenz et al., 2010; Guo et al., 2012; Huang, 2013; Huang et al., 2013). Although the river plume's influence on the CO_2 flux has been addressed by observational studies, large uncertainties, mainly resulting from the relatively sporadic measurement, were also found regarding whether the Louisiana Shelf is a CO_2 sink or source over a longer time period. For instance, Huang et al. (2013) found a large difference between the $p\text{CO}_2$ distributions in April 2009 and in March 2010, which was attributed to the variations in river plume extent influenced by different local wind conditions.

Model results in this study reveal significant spatial and temporal gradients in $p\text{CO}_2$ as well. Our model-simulated multi-year mean (2005–2010) distribution of $p\text{CO}_2$ was characterized by relatively high values in the coastal waters on the Louisiana Shelf (Fig. 3a) accompanied by low salinities (Fig. 3c), high DIN and high DIC (Fig. 3d and e). In contrast, the $p\text{CO}_2$ value on the open shelf was significantly lower, thus making it a CO_2 sink during most time of the year (Fig. 2a–d). On the shelf-scale the $p\text{CO}_2$ distribution was highly correlated with surface salinity (r value: -0.81) and DIN concentration (r value: 0.80) throughout the year, while relationships to surface temperature and DIC concentration were significant only for part of the year (detailed season-by-season correlation see Table 2). Previous studies have reported that during high flow seasons, high concentrations of nutrients in the plume water stimulate primary production, resulting in a $p\text{CO}_2$ removal through the biological pump (e.g., Lohrenz et al., 2010), which was confirmed by the elevated $p\text{CO}_2$ value in the no-bio simulation in this study. Although our model suggests that on the Louisiana Shelf the $p\text{CO}_2$ distribution was positively correlated with DIN concentration, this is not contrary to findings of

12682

the above-mentioned observational studies; the high DIN concentration, together with the low salinity, is a signal of the river plume. In other words, on a yearly scale model results indicate the spatial distribution of surface $p\text{CO}_2$ is mostly dominated by the extent of the oversaturated plume water (low salinity and high DIN), which degases more CO_2 despite high primary production. This also explains why our model suggests the Louisiana Shelf is a CO_2 source instead of a sink during summer months when primary production is high (Table 1 and Fig. 2). However, caution should be taken as our model seems to overestimate surface $p\text{CO}_2$ during summer months (Fig. 1a), which can be attributed to: (1) the spatial and temporal heterogeneity of the in situ measurements, (2) current model solution (~ 5 km) may not be high enough to reproduce small scale circulation patterns associated with the Mississippi River plume; and (3) the complexity of the food web and uncertainty in model parameterization (e.g. rudimentarily represented particular organic matters, the lack of phosphate and silicate components, etc.).

In the open ocean, the distribution of surface $p\text{CO}_2$ is largely determined by that of DIC (r value: 0.96) and alkalinity throughout the year (r value: -0.81 , detailed season-by-season correlation see Table 2), while the influence from DIN and primary production is limited to fall and winter months when wind-induced upwelling is strong (Xue et al., 2013 and references therein). The dependence of $p\text{CO}_2$ on DIC and alkalinity makes the transport of water from the Caribbean Sea through the Yucatan Channel an important factor in the regional air–sea CO_2 flux. In addition to high temperature, the Caribbean waters are also characterized by low DIC and high alkalinity (Wang et al., 2013 and references therein). In the GoM, the multi-year mean sea surface temperature shows a persistent warm water mass in the form of the LC (Fig. 3b), which carries the signal of carbonate characteristics of Caribbean water (i.e. low DIC and high alkalinity, Fig. 3e and f). Surface $p\text{CO}_2$ in this warm water mass is significantly lower than in the surrounding waters (Fig. 3a), making the Loop Current a strong carbon sink throughout the year (Fig. 2a–d). In other words, any changes in the Caribbean water's

12683

carbonate characteristics will affect the carbon budget in the GoM as well as waters further downstream along the Gulf Stream.

4.2 Uncertainty in carbon budget estimation

Based on our model-simulations, we conclude that the GoM is an overall CO_2 sink, taking up $1.34 \times 10^{12} \text{ mol C yr}^{-1}$ from the air. This estimation is comparable to those based on in situ observations, e.g. $1.48 \times 10^{12} \text{ mol C yr}^{-1}$, (Coble et al., 2010) and $0.30 \times 10^{12} \text{ mol C yr}^{-1}$ (Robbins et al., 2014). These recent estimates are in stark contrast to the earlier SOCCR report (Takahashi et al., 2007), which found the GoM to be a CO_2 source ($1.58 \times 10^{12} \text{ mol C yr}^{-1}$, the GoM and Caribbean Sea combined). In addition, we estimate that the GoM receives $\sim 2.18 \times 10^{12} \text{ mol C yr}^{-1}$ from rivers ($\sim 1.80 \times 10^{12} \text{ mol C yr}^{-1}$ from the Mississippi/Atchafalaya River). These two DIC sources (air: $\sim 1.34 \times 10^{12} \text{ mol C yr}^{-1}$ plus river: $\sim 2.18 \times 10^{12} \text{ mol C yr}^{-1}$) largely balance the DIC transported out of the GoM by the Loop Current ($\sim 3.30 \times 10^{12} \text{ mol C yr}^{-1}$, Wang et al., 2013).

We note that although the model generates estimates of the DIC flux through the Yucatan Channel and Florida Straits, large uncertainties remain with regard to quantifying the DIC concentration in the water column. Similar to the situation reported by Hofmann et al. (2011), we found the model-simulated DIC concentration in the water column to be very sensitive to the initial conditions. Although there are historical measurements in the GoM, the majority of these data are limited to the Louisiana Shelf. In our model, we calculated the initial and open boundary conditions of DIC and alkalinity for the open ocean using the empirical relationship in Lee et al. (2000 and 2006), which was derived based on measurements of the surface ocean. In addition, the large gradient in observed $p\text{CO}_2$ in the shallow water as well as the discrepancy between simulated and observed values during summer months on the Louisiana Shelf warrants further investigation.

12684

5 Summary

A coupled physical–biogeochemical model was used to hindcast surface $p\text{CO}_2$ in the GoM from January 2004 to December 2010. Favorable comparisons were found when validating model solutions against in situ measurements on a gulf-wide extent, indicating that this coupled model can reproduce observed $p\text{CO}_2$ variability in the GoM. Time series of spatially averaged $p\text{CO}_2$ for both shelf and open ocean waters exhibit significant seasonal variability, with high values in August and low values in February. Model simulated $p\text{CO}_2$ is elevated by ~ 70 ppm when the biological sources and sinks of carbon were disabled (i.e., the no-bio simulation) and the GoM shifted to a strong carbon source with a outflux of $1.57 \text{ mol C m}^{-2} \text{ yr}^{-1}$. Model-estimated air–sea CO_2 flux exhibited large spatial variability as well, with highest $p\text{CO}_2$ on the Louisiana shelf. While the Mississippi/Atchafalaya River plume is the dominant factor controlling the $p\text{CO}_2$ distribution on the Louisiana Shelf, $p\text{CO}_2$ in the open ocean is controlled mostly by DIC and alkalinity throughout the year as well as DIN and associated primary production during fall and winter months.

Our model simulations characterize the GoM as an overall CO_2 sink, taking up $\sim 1.34 \times 10^{12} \text{ mol C yr}^{-1}$ from the air. Together with the enormous riverine input ($\sim 2.18 \times 10^{12} \text{ mol C yr}^{-1}$), this carbon influx is largely balanced by carbon export through the Loop Current in agreement with estimates from previous observational studies. More accurate model predictions of water column DIC concentration will require more in-situ data for improved specification of model DIC initial conditions, and better model parameterizations accounting for complex carbon dynamics around the Mississippi River plume.

Acknowledgements. Research support provided through the National Aeronautics and Space Administration (NNX10AU06G and NNX12AP84G); National Science Foundation (OCE-0752254 and OCE-0752110); NOAA Grant NA11NOS0120033; and GRI GISR grant SA/GoMRI-006 and GOMRI-020 is much appreciated. The operational mode of the SABGOM model is located at <http://omgsrv1.meas.ncsu.edu:8080/ocean-circulation/>. Data of daily now-cast/forecast model output is hosted at http://omgsrv1.meas.ncsu.edu:8080/thredds/sabgom_12685

12685

catalog.html. Data used in all figures for the hindcast simulation can be obtained by contacting the corresponding author.

References

- Aulenbach, B. T., Buxton, H. T., Battaglin, W. T., and Coupe, R. H.: Streamflow and nutrient fluxes of the Mississippi–Atchafalaya River Basin and subbasins for the period of record through 2005, US Geological Survey Open-File Report 2007-1080 Rep., 2007.
- Bauer, J. E., Cai, W.-J., Raymond, P. A., Bianchi, T. S., Hopkinson, C. S., and Regnier, P. A. G.: The changing carbon cycle of the coastal ocean, *Nature*, 504, 61–70, 2013.
- Benway, H. M. and Coble, P. G.: Introduction, Report of The US Gulf of Mexico Carbon Cycle Synthesis Workshop, Ocean Carbon and Biogeochemistry Program and North American Carbon Program Rep, 63 pp., 2014.
- Cai, W.-J.: Riverine inorganic carbon flux and rate of biological uptake in the Mississippi River plume, *Geophys. Res. Lett.*, 30, 1032, doi:10.1029/2002GL016312, 2003.
- Cai, W.-J.: Estuarine and coastal ocean carbon paradox: CO_2 sinks or sites of terrestrial carbon incineration?, *Annu. Rev. Mar. Sci.*, 3, 123–145, 2011.
- Cai, W.-J., Hu, X., Huang, W.-J., Murrell, M. C., Lehrter, J. C., Lohrenz, S. E., Chou, W.-C., Zhai, W., Hollibaugh, J. T., Wang, Y., Zhao, P., Guo, X., Gundersen, K., Dai, M., and Gong, G.-C.: Acidification of subsurface coastal waters enhanced by eutrophication, *Nat. Geosci.*, 4, 766–770, 2011.
- Chassignet, E. P., Hurlburt, H. E., Smedstad, O. M., Halliwell, G. R., Hogan, P. J., Wallcraft, A. J., Baraille, R., and Bleck, R.: The HYCOM (HYbrid Coordinate Ocean Model) data assimilative system, *J. Marine Syst.*, 65, 60–83, 2007.
- Chavez, F. P., Takahashi, T., Cai, W. J., Friederich, G., Hales, B., Wanninkhof, R., and Feely, R. A.: Coastal Oceans Rep., National Climatic Data Center, Asheville, NC, USA, 2007.
- Coble, P. G., Robbins, L. L., Daly, K. L., Cai, W. J., Fennel, K., and Lohrenz, S. E.: A preliminary carbon budget for the Gulf of Mexico, *Ocean Carbon and Biogeochemistry News*, 3, 1–4, 2010.
- Feely, R. A., Sabine, C. L., Lee, K., Berelson, W., Kleypas, J., Fabry, V. J., and Millero, F. J.: Impact of anthropogenic CO_2 on the CaCO_3 system in the oceans, *Science*, 305, 362–366, 2004.

- Fennel, K.: The role of continental shelves in nitrogen and carbon cycling: Northwestern North Atlantic case study, *Ocean Sci.*, 6, 539–548, 2010, <http://www.ocean-sci.net/6/539/2010/>.
- Fennel, K. and Wilkin, J.: Quantifying biological carbon export for the northwest North Atlantic continental shelves, *Geophys. Res. Lett.*, 36, L18605, doi:10.1029/2009GL039818, 2009.
- 5 Fennel, K., Wilkin, J., Levin, J., Moisan, J., O'Reilly, J., and Haidvogel, D. B.: Nitrogen cycling in the Middle Atlantic Bight: results from a three-dimensional model and implications for the North Atlantic nitrogen budget, *Global Biogeochem. Cy.*, 20, GB3007, doi:10.1029/2005GB002456, 2006.
- 10 Fennel, K., Wilkin, J., Previdi, M., and Najjar, R.: Denitrification effects on air–sea CO₂ flux in the coastal ocean: simulations for the Northwest North Atlantic, *Geophys. Res. Lett.*, 35, L24608, doi:10.1029/2008GL036147, 2008.
- Fennel, K., Hetland, R., Feng, Y., and DiMarco, S.: A coupled physical-biological model of the Northern Gulf of Mexico shelf: model description, validation and analysis of phytoplankton variability, *Biogeosciences*, 8, 1881–1899, doi:10.5194/bg-8-1881-2011, 2011.
- 15 Fuentes-Yaco, C., de Leon, D. A. S., Monreal-Gomez, M. A., and Vera-Herrera, F.: Environmental forcing in a tropical estuarine ecosystem: the Palizada River in the southern Gulf of Mexico, *Mar. Freshwater Res.*, 52, 735–744, 2001.
- Gledhill, D. K., Wanninkhof, R., Millero, F. J., and Eakin, M.: Ocean acidification of the Greater Caribbean Region 1996–2006, *J. Geophys. Res.-Oceans*, 113, C10031, doi:10.1029/2007JC004629, 2008.
- 20 Guo, X., Cai, W.-J., Huang, W.-J., Wang, Y., Chen, F., Murrell, M. C., Lohrenz, S. E., Jiang, L.-Q., Dai, M., Hartmann, J., Lin, Q., and Culp, R.: Carbon dynamics and community production in the Mississippi River plume, *Limnol. Oceanogr.*, 57, 1–17, 2012.
- 25 Haidvogel, D. B., Arango, H., Budgell, W. P., Cornuelle, B. D., Curchitser, E., Di Lorenzo, E., Fennel, K., Geyer, W. R., Hermann, A. J., Lanerolle, L., Levin, J., McWilliams, J. C., Miller, A. J., Moore, A. M., Powell, T. M., Shchepetkin, A. F., Sherwood, C. R., Signell, R. P., Warner, J. C., and Wilkin, J.: Ocean forecasting in terrain-following coordinates: formulation and skill assessment of the Regional Ocean Modeling System, *J. Comput. Phys.*, 227, 3595–3624, 2008.
- 30 Hofmann, E. E., Cahill, B., Fennel, K., Friedrichs, M. A., Hyde, K., Lee, C., Mannino, A., Najjar, R. G., O'Reilly, J. E., and Wilkin, J.: Modeling the dynamics of continental shelf carbon, *Annu. Rev. Mar. Sci.*, 3, 93–122, 2011.

12687

- Huang, W.-J.: Inorganic Carbon Distribution and Dynamics in the Mississippi River Plume on the Northern Gulf of Mexico, University of Georgia, Athens, GA, 2013.
- Huang, W.-J., Cai, W. J., Castelao, R., W. Y., and Lohrenz, S. E.: Effects of a wind-driven cross-shelf large river plume on biological production and CO₂ uptake on the Gulf of Mexico during spring, *Limnol. Oceanogr.*, 58, 1727–1735, 2013.
- 5 IPCC: Climate Change 2001: The Scientific Basis, Cambridge University Press, 2001.
- Jiang, L. Q., Cai, W. J., Wanninkhof, R., Wang, Y. C., and Luger, H.: Air–sea CO₂ fluxes on the US South Atlantic Bight: spatial and seasonal variability, *J. Geophys. Res.-Oceans*, 113, C07019, doi:10.1029/2007JC004366, 2008.
- 10 Lee, K., Wanninkhof, R., Feely, R. A., Millero, F. J., and Peng, T.-H.: Global relationships of total inorganic carbon with temperature and nitrate in surface seawater, *Global Biogeochem. Cy.*, 14, 979–994, doi:10.1029/1998GB001087, 2000.
- Lee, K., Tong, L. T., Millero, F. J., Sabine, C. L., Dickson, A. G., Goyet, C., Park, G. H., Wanninkhof, R., Feely, R. A., and Key, R. M.: Global relationships of total alkalinity with salinity and temperature in surface waters of the world's oceans, *Geophys. Res. Lett.*, 33, L19605, doi:10.1029/2006GL027207, 2006.
- 15 Lohrenz, S. E., Cai, W. J., Chen, F. Z., Chen, X. G., and Tuel, M.: Seasonal variability in air–sea fluxes of CO₂ in a river-influenced coastal margin, *J. Geophys. Res.-Oceans*, 115, C10034, doi:10.1029/2009JC005608, 2010.
- 20 Milliman, J. D. and Farnsworth, K. L.: River Discharge to the Coastal Ocean: a Global Synthesis, Cambridge University Press, Cambridge, New York, 384 pp., 2011.
- Murrell, M. C., Stanley, R. S., and Lehrter, J. C.: Plankton community respiration, net ecosystem metabolism, and oxygen dynamics on the Louisiana continental shelf: implications for hypoxia, *Cont. Shelf. Res.*, 52, 27–38, 2013.
- 25 Nixon, S. W., Ammerman, J. W., Atkinson, L. P., Berounsky, V. M., Billen, G., Boicourt, W. C., Boynton, W. R., Church, T. M., Ditoro, D. M., Elmgren, R., Garber, J. H., Giblin, A. E., Jahnke, R. A., Owens, N. J. P., Pilson, M. E. Q., and Seitzinger, S. P.: The fate of nitrogen and phosphorus at the land sea margin of the North Atlantic Ocean, *Biogeochemistry*, 35, 141–180, 1996.
- 30 Orr, J. C., Najjar, R., Sabine, C. L., and Joos, F.: OCMIP Abiotic-HOWTO, available at: <http://ocmip5.ipsl.jussieu.fr/OCMIP/phase1/>, 2000.
- Orr, J. C., Fabry, V. J., Aumont, O., Bopp, L., Doney, S. C., Feely, R. A., Gnanadesikan, A., Gruber, N., Ishida, A., Joos, F., Key, R. M., Lindsay, K., Maier-Reimer, E., Matear, R., Monfray,

12688

- P., Mouchet, A., Najjar, R. G., Plattner, G.-K., Rodgers, K. B., Sabine, C. L., Sarmiento, J. L., Schlitzer, R., Slater, R. D., Totterdell, I. J., Weirig, M.-F., Yamanaka, Y., and Yool, A.: Anthropogenic ocean acidification over the twenty-first century and its impact on calcifying organisms, *Nature*, 437, 681–686, 2005.
- 5 Rabalais, N., Turner, R. E., and Wiseman, W. J. J.: Gulf of Mexico Hypoxia, a.k.a. the Dead Zone, *Annu. Rev. Ecol. Syst.*, 33, 235–263, 2002.
- Robbins, L. L., Wanninkhof, R., Barbero, L., Hu, X., Mitra, S., Yvon-Lewis, S., Cai, W., Huang, W., and Ryerson, T.: Air–Sea Exchange, Report of The US Gulf of Mexico Carbon Cycle Synthesis Workshop, Ocean Carbon and Biogeochemistry Program and North American Carbon Program Rep., 63 pp., 2014.
- 10 Sabine, C. L. and Tanhua, T.: Estimation of anthropogenic CO₂ inventories in the ocean, *Annu. Rev. Mar. Sci.*, 2, 175–198, 2010.
- Sabine, C. L., Feely, R. A., Gruber, N., Key, R. M., Lee, K., Bullister, J. L., Wanninkhof, R., Wong, C. S., Wallace, D. W. R., Tilbrook, B., Millero, F. J., Peng, T. H., Kozyr, A., Ono, T., and Rios, A. F.: The oceanic sink for anthropogenic CO₂, *Science*, 305, 367–371, 2004.
- 15 Shchepetkin, A. F. and McWilliams, J. C.: The Regional Ocean Modeling System (ROMS): a split-explicit, free-surface, topography-following coordinates ocean model, *Ocean Model.*, 9, 347–404, 2005.
- Signorini, S. R., Mannino, A., Najjar, R. G., Friedrichs, M. A. M., Cai, W.-J., Salisbury, J., Wang, Z. A., Thomas, H., and Shadwick, E.: Surface ocean pCO₂ seasonality and sea–air CO₂ flux estimates for the North American east coast, *J. Geophys. Res.-Oceans*, 118, 5439–5460, doi:10.1002/jgrc.20369, 2013.
- 20 Sturges, W. and Leben, R.: Frequency of ring separations from the loop current in the Gulf of Mexico: a revised estimate, *J. Phys. Oceanogr.*, 30, 1814–1819, 2000.
- 25 Takahashi, T., Sutherland, S. C., and Kozyr, A.: Global Ocean Surface Water Partial Pressure of CO₂ Database: Measurements Performed During 1957–2012 (Version 2012) Rep., Carbon Dioxide Information Analysis Center, Oak Ridge National Laboratory, US Department of Energy, Oak Ridge, Tennessee, 2013.
- Toner, M., Kirwan, A. D., Poje, A. C., Kantha, L. H., Muller-Karger, F. E., and Jones, C. K. R. T.: Chlorophyll dispersal by eddy–eddy interactions in the Gulf of Mexico, *J. Geophys. Res.-Oceans*, 108, 3105, doi:10.1029/2002JC001499, 2003.
- 30 Tsunogai, S., Watanabe, S., and Sato, T.: Is there a “continental shelf pump” for the absorption of atmospheric CO₂?, *Tellus B*, 51, 701–712, 1999.

12689

- Wang, Z. A., Wanninkhof, R., Cai, W.-J., Byrne, R. H., Hu, X., Peng, T.-H., and Huang, W.-J.: The marine inorganic carbon system along the Gulf of Mexico and Atlantic coasts of the United States: insights from a transregional coastal carbon study, *Limnol. Oceanogr.*, 58, 325–342, 2013.
- 5 Wanninkhof, R.: Relationship between wind-speed and gas-exchange over the ocean, *J. Geophys. Res.-Oceans*, 97, 7373–7382, doi:10.1029/92JC00188, 1992.
- Xue, Z., He, R., Fennel, K., Cai, W.-J., Lohrenz, S., and Hopkinson, C.: Modeling ocean circulation and biogeochemical variability in the Gulf of Mexico, *Biogeosciences*, 10, 7219–7234, doi:10.5194/bg-10-7219-2013, 2013.
- 10 Zeebe, R. and Wolf-Gladrow, D.: CO₂ in Seawater: Equilibrium, Kinetics, Isotopes, Elsevier, Amsterdam, 2001.

12690

Table 1. Multi-year mean (2005–2010) of model-simulated air–sea CO₂ flux against the estimation based on in situ measurements^a.

		Sub-regions					Gulf-wide ^b
		Mexico Shelf	Texas Shelf	Louisiana Shelf	West Florida Shelf	Open Ocean	
Subregion Area (10 ¹² m ²)		0.18	0.08	0.15	0.15	1.01	1.56
Model (control run) ^a	Spring	1.76	−0.03	0.99	0.49	1.36	1.23
	Summer	0.03	−1.15	−1.47	−1.06	−0.09	−0.39
	Fall	0.31	−0.46	−0.41	−1.28	0.81	0.42
	Winter	2.25	1.89	2.59	1.41	2.24	2.19
	Annual	1.09	0.06	0.42	−0.11	1.06	0.86
Observation^c	Annual	0.09	0.18	0.44	−0.37	0.48	0.19
Model (no-bio simulation)	Annual	−1.43	−1.28	−0.97	−1.06	−1.75	−1.57

^a Unit: mol m^{−2} yr^{−1}, + indicates ocean is a CO₂ sink.^b Gulf-wide value is a sum of all sub-regions.^c From Robbins et al. (2014).

12691

Table 2. Spatial correlation coefficients between pCO₂, sea surface temperature (SST), sea surface salinity (SSS), dissolved inorganic nitrate (DIN: NO₃ + NH₄), dissolved inorganic carbon (DIC), alkalinity (ALK), and primary production (P-Prod) on the Louisiana Shelf and in the open ocean (multi-year mean of 2005–2010, control run).

Correlation Coefficient (<i>R</i> value)		SST	SSS	DIC	DIN	ALK	P-Prod
pCO ₂ on the Louisiana Shelf	Spring	−0.23	−0.81	−0.03	0.84	−0.79	0.38
	Summer	0.67	−0.60	0.67	0.65	−0.23	0.37
	Fall	−0.72	−0.88	0.86	0.73	−0.04	0.55
	Winter	−0.74	−0.87	0.51	0.86	−0.90	0.22
	Annual	−0.69	−0.81	0.66	0.80	−0.68	0.47
pCO ₂ in open ocean	Spring	−0.03	0.06	0.87	−0.25	−0.73	−0.38
	Summer	−0.18	−0.16	0.99	−0.34	−0.82	−0.39
	Fall	−0.03	0.01	0.98	−0.79	−0.82	−0.78
	Winter	−0.16	−0.14	0.88	−0.53	−0.76	−0.62
	Annual	−0.25	−0.04	0.96	−0.52	−0.81	−0.60

12692

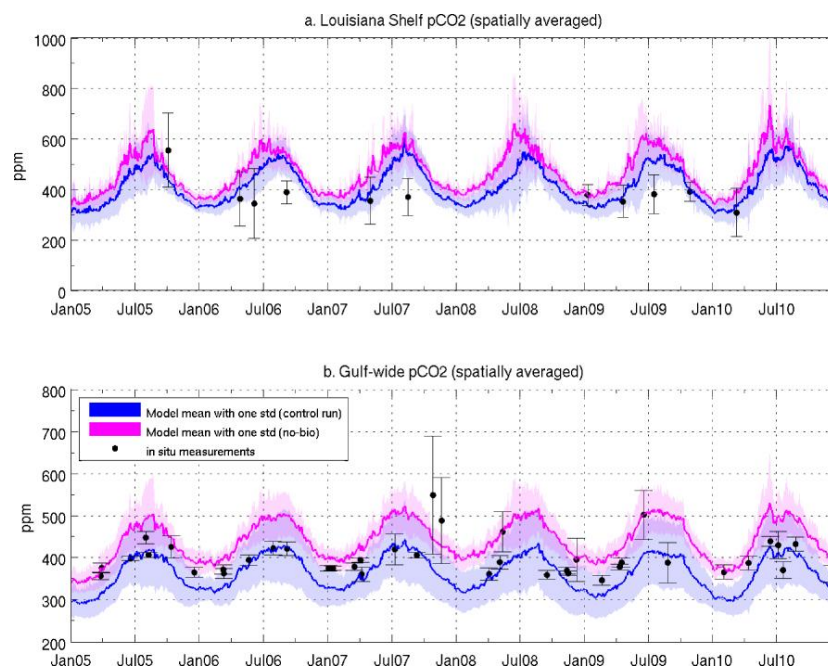


Figure 1. Time series of spatially averaged $p\text{CO}_2$ (control run in pink and no-bio simulation in blue) **(a)** on the Louisiana shelf, and **(b)** in the entire Gulf of Mexico, overlaid with in situ observations (in red) from Huang (2013), Huang et al. (2013), and Takahashi et al. (2013).

12693

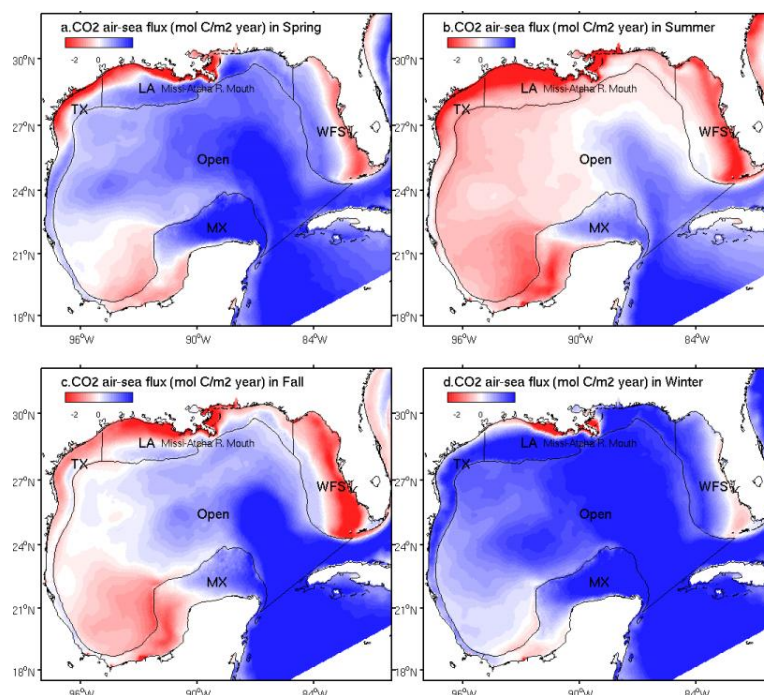


Figure 2. Multi-year mean (2005–2010) of model-simulated air-sea CO_2 flux in the Gulf of Mexico (control run) during **(a)** spring, **(b)** summer, **(c)** autumn, and **(d)** winter. Blue color indicates where the ocean is a sink for CO_2 ; red color indicates where the ocean is a source. TX = Texas Shelf, LA = Louisiana Shelf, WFS = West Florida Shelf, MX = Mexico Shelf, and Open = open ocean.

12694

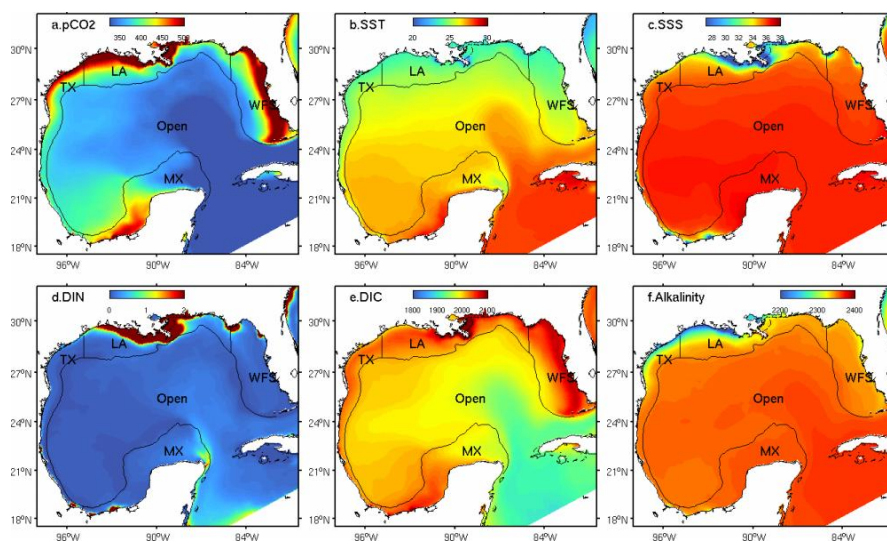


Figure 3. Multi-year mean (2005–2010) conditions simulated by the model for **(a)** $p\text{CO}_2$ (ppm), **(b)** sea surface temperature (degree C), **(c)** sea surface salinity (psu), **(d)** dissolved inorganic nitrogen ($\text{NO}_3 + \text{NH}_4$) (mmol N m^{-3}), **(e)** dissolved inorganic carbon (mmol C m^{-3}), and **(f)** alkalinity (mEq m^{-3}).